Small Molecule Therapeutics

Molecular Cancer Therapeutics

Targeting 6-Phosphofructo-2-Kinase (PFKFB3) as a Therapeutic Strategy against Cancer

Brian F. Clem[1], Julie O'Neal[1], Gilles Tapolsky[2], Amy L. Clem[1], Yoannis Imbert-Fernandez[1], Daniel A. Kerr II[1], Alden C. Klarer[1], Rebecca Redman[1], Donald M. Miller[1], John O. Trent[1], Sucheta Telang[1], and Jason Chesney[1]

Abstract

In human cancers, loss of *PTEN*, stabilization of hypoxia inducible factor-1α, and activation of Ras and AKT converge to increase the activity of a key regulator of glycolysis, 6-phosphofructo-2-kinase (PFKFB3). This enzyme synthesizes fructose 2,6-bisphosphate (F26BP), which is an activator of 6-phosphofructo-1-kinase, a key step of glycolysis. Previously, a weak competitive inhibitor of PFKFB3, 3-(3-pyridinyl)-1-(4-pyridinyl)-2-propen-1-one (3PO), was found to reduce the glucose metabolism and proliferation of cancer cells. We have synthesized 73 derivatives of 3PO and screened each compound for activity against recombinant PFKFB3. One small molecule, 1-(4-pyridinyl)-3-(2-quinolinyl)-2-propen-1-one (PFK15), was selected for further preclinical evaluation of its pharmacokinetic, antimetabolic, and antineoplastic properties *in vitro* and *in vivo*. We found that PFK15 causes a rapid induction of apoptosis in transformed cells, has adequate pharmacokinetic properties, suppresses the glucose uptake and growth of Lewis lung carcinomas in syngeneic mice, and yields antitumor effects in three human xenograft models of cancer in athymic mice that are comparable to U.S. Food and Drug Administration–approved chemotherapeutic agents. As a result of this study, a synthetic derivative and formulation of PFK15 has undergone investigational new drug (IND)-enabling toxicology and safety studies. A phase I clinical trial of its efficacy in advanced cancer patients will initiate in 2013 and we anticipate that this new class of antimetabolic agents will yield acceptable therapeutic indices and prove to be synergistic with agents that disrupt neoplastic signaling. *Mol Cancer Ther; 12(8); 1461–70. ©2013 AACR.*

Introduction

Increased glucose uptake and metabolism are required for neoplastic cells to survive and proliferate within the microenvironment of a tumor. This nearly ubiquitous characteristic of human cancers forms the basis of a clinically useful diagnostic imaging modality that depends on the detection of pairs of γ rays emitted indirectly by positron-emitting 2-deoxy-2-[^{18}F]fluoro-D-glucose consumed by tumor cells (i.e., ^{18}FDG-PET imaging; refs. 1 and 2). The mechanisms that drive increased glucose uptake and metabolism in tumors include a combination of the survival response to hypoxia via the transcription factor, hypoxia inducible factor-1α (HIF-1α; ref. 3), as well as genetic alterations such as amplification of c-*MYC* that can independently increase the expression and activities of multiple glucose transporters and glycolytic enzymes, including the Glut1 glucose transporter, hexokinase 2, 6-phosphofructo-1-kinase (PFK-1), pyruvate kinase M2, and lactate dehydrogenase A (4–6). Of these enzymes, PFK-1 is of particular interest because this irreversible and committed step of glycolysis serves as a metabolic sensor for the entire pathway via its allosteric inhibition by ATP, citrate, and H+ ions (7, 8).

In the late 1970s, a novel allosteric activator of PFK-1, fructose 2,6-bisphosphate (F26BP), was discovered that could override the inhibition by ATP and increase glucose uptake and flux through the entire glycolytic pathway (7, 9). A family of 5 enzymes (PFKFB1-4, TIGAR) regulates the intracellular concentration of F26BP via a combination of fructose 6-phosphate kinase and F26BP phosphatase activities (8). Although the expression of most of these regulatory enzymes is increased by hypoxia (10), the PFKFB3 family member has been found to be a direct transcriptional target of HIF-1α (11), to be stabilized by the loss of the tumor suppressor *PTEN* via suppressive effects on APC/Cdh1-mediated ubiquitination (12), and to be activated by oncogenic Ras and AKT (13, 14). Importantly, PFKFB3 protein expression is elevated in most tumor types (15) and heterozygous genomic deletion of the *Pfkfb3* gene markedly reduces the concentration of F26BP, glucose uptake, glycolytic flux to lactate, and anchorage-independent growth of LT/H-Ras^{V12}-transformed fibroblasts as soft agar colonies and as xenograft tumors in syngeneic mice (14, 16). Coupled to recent data, which

Authors' Affiliations: [1]Division of Medical Oncology and Hematology, Department of Medicine, University of Louisville, James Graham Brown Cancer Center; and [2]Advanced Cancer Therapeutics, Louisville, Kentucky

B.F. Clem and J. O'Neal contributed equally to this article.

Corresponding Author: Jason Chesney, University of Louisville, 505 South Hancock Street, Clinical and Translational Research Building Room 424, University of Louisville, Louisville, KY 40202. Phone: 502-852-3402; Fax: 502-852-3661; E-mail: jason.chesney@louisville.edu

doi: 10.1158/1535-7163.MCT-13-0097

indicate that PFKFB3 is not expressed by primary neurons that, like neoplastic cells, have a very high rate of glucose uptake and metabolism (17), these studies indicate that small molecule inhibitors of PFKFB3 may have utility as anticancer agents.

A small molecule antagonist of PFKFB3, 3-(3-pyridinyl)-1-(4-pyridinyl)-2-propen-1-one (3PO), was recently identified using a combination of computational modeling and receptor based *in silico* screening (18). 3PO causes a rapid reduction in F26BP, glucose uptake, and lactate secretion followed by a reduction in the steady-state concentration of ATP and NADH, and an arrest in cell-cycle progression in Jurkat T-cell leukemia cells (18). Although this compound exhibits antitumor activity in mice (18), its pharmacokinetic properties and potency against the enzymatic activity of PFKFB3 are significantly below that required to justify testing in human subjects. In this study, we synthesized multiple derivatives of 3PO to improve the pharmacokinetic properties and activity of 3PO and now report the identification of a novel PFKFB3 inhibitor termed PFK15 that has potent antitumor activity and that markedly reduces ^{18}FDG uptake and the F26BP content of xenografted tumors. We also show for the first time that this novel class of antineoplastic agents has potent and rapid pro-apoptotic effects on transformed cells *in vitro* and in tumors *in vivo*.

Materials and Methods

Recombinant PFKFB3 assay

Kinase reactions were conducted by incubating 13 ng of recombinant human PFKFB3 protein in a reaction mix containing 10 μmol/L ATP, 10 μmol/L F6P, and either dimethyl sulfoxide (DMSO) vehicle control, 3PO, or PFK15 for 1 hour at room temperature. Kinase activity was measured with the Adapta Universal Kinase Assay (Invitrogen) per manufacturer's instructions and fluorescent and FRET signals were measured on a Tecan Safire^2 plate reader. Graphs were generated using SigmaPlot software and IC_{50} values were calculated using a 3-parameter Hill Equation. The KINOMEscanEDGE list of 96 kinases can be accessed at http://www.kinomescan.com.

Cell lines and culture

Lewis lung carcinoma (LLC), Jurkat T-cell leukemia cells, H522 human lung adenocarcinoma cells, CT26 colon adenocarcinoma cells, U-87 glioblastoma cells, and BxPC-3 pancreatic cancer cells were maintained in RPMI or Dulbecco's modified Eagle medium supplemented with 10% fetal calf serum (FCS; HyClone), glucose (20 mmol/L), and glutamine (1 mmol/L). The cell lines were obtained from the American Type Culture Collection (ATCC, Manassas, VA) and passaged for fewer than 6 months after receipt or resuscitation. ATCC conducted authentication of cell lines using a combination of sequencing, short tandem repeat profiling, and cytogenetic analysis. The morphology and behavior of each line were consistent with ATCC descriptions. Cells were plated at a density of 1×10^5 cells/well in 6-well tissue culture plates and incubated in RPMI or DMEM for 24 hours (5% CO_2 and 37°C). Cells then were exposed to 3PO (Chembridge) or PFK15 (Advanced Cancer Therapeutics) at the indicated concentrations and assayed for viability (48 hours), F26BP (3 hours), glucose uptake (3 hours), and intracellular ATP (3 hours). Experiments were conducted in triplicate or quadruplicate and statistical significance was assessed by the unpaired 2-tailed *T* test.

Cell viability

Viability was determined using trypan blue exclusion. Cells were incubated in 20% trypan blue (Sigma) for 5 minutes. Cells excluding trypan blue were counted using a standard hemocytometer (Hausser Scientific) to determine the total number of viable cells. Experiments were conducted in triplicate.

F26BP measurements

Cells were triturated, washed twice with PBS, dissolved in 0.1 mmol/L NaOH and 50 mmol/L Tris Acetate, and F26BP content measured using a coupled enzyme reaction following the method of Van Schaftingen and colleagues (7). The F26BP concentration was normalized to total cellular protein measured by the Bradford assay (Pierce Biotechnology).

2-[1-^{14}C]-deoxy-D-glucose uptake

Jurkat or H522 cells were plated in RPMI 1640 media supplemented with 10% FCS and 50 μg/mL gentamycin at 100,000/mL and immediately treated with DMSO vehicle control, 3PO, or PFK15 for 3 hours. Cells were washed twice with prewarmed glucose-free RPMI media and incubated for 30 minutes in the presence of the PFKFB3 inhibitors. Cells were treated with 25 μL of ^{14}C-deoxyglucose (0.1 μCi/μL) for 1 hour, washed once with ice-cold glucose-free RPMI and twice with ice cold PBS. Cells were lysed in 500 μL 0.5% SDS. Four hundred microliters of lysate was added to 5 mL Microscint 40 scintillation fluid (Perkin-Elmer) and counts were measured on a Tri-Carb 2910 liquid scintillation analyzer (Perkin-Elmer). Remaining lysate was quantitated with the BCA Assay (Pierce) per manufacturer's instructions and protein levels measured on a Powerwave XS plate reader (Biotek). Counts were normalized to protein concentration.

ATP assay

Cells were washed (while still adherent) with cold PBS 1×, lysed with passive lysis buffer (1×; Molecular Probes, Invitrogen), added directly to the plates, and immediately harvested by scraping. The lysates were flash frozen (to −80°C) and thawed (to 37°C) once to accomplish complete lysis and then centrifuged (at 4°C) for 30 seconds to clear the lysates. Intracellular ATP levels were determined using a bioluminescence assay (Molecular Probes), utilizing recombinant firefly luciferase and its substrate, D-luciferin. The luminescence was read in a TD-20/20 luminometer (Turner Designs) at 560 nm. The ATP values were calculated using an

ATP standard curve. The protein concentrations of the lysates were estimated using the BCA assay (Pierce Biotechnology) and ATP was expressed as nmol per mg protein.

Flow cytometry

Jurkat cells were plated in RPMI 1640 media supplemented with 10% FCS and 50 μg/mL gentamycin at 100,000 cells/mL and immediately incubated with DMSO vehicle control, 3PO, PFK15, or Etoposide (Sigma) for 5 hours. Cells were washed with PBS and stained with Annexin V and propidium iodide (PI; BD Pharmingen). Fluorescence was measured using a FACSCalibur (BD Biosciences) and analyzed using FloJo (Tree Star). Annexin V+/PI+ (late apoptotic) and Annexin V+/PI− (early apoptotic) cells were quantified by the frequency of fluorescently labeled cells and statistical significance was assessed by the 2-sample *T* test (independent variable).

Pharmacokinetic studies

The pharmacokinetics (PK) profile was determined in female C57Bl/6 mice after i.v. administration of the PFKFB3 inhibitors. Using only female mice lowered the number of animals required for meaningful results without the issues of potential gender differences in exposure. A total of 8 time points and 3 animals per time point were used to determine the PK parameters calculated using WinNonLin v5.0 [T_{max}, C_{max}, volume of distribution, half-life, clearance, area under curves (AUC), and mean residence time (MRT)]. Plasma samples were extracted using acetonitrile and analyzed by LC/MS-MS using a Phenomex Synergi Polar-RP 4 μm 50 × 2.0 mm column eluted with a biphasic mobile phase (0.5% formic acid in acetonitrile and water).

FDG-PET imaging

Tumor-bearing mice were anesthetized with isoflurane and 200 μCi of FDG was administered i.v. via the tail veins. The baseline micro-PET imaging of FDG in the mice was acquired by the ordered subsets expectation maximization, using 6 subsets/4 iterations for 15-minute static scans 45 minutes after i.v. injection of the tracer using a Concorde Microsystems 4-ring micro-PET system. Regions of interest in the tumor and cerebellum were quantified in quadruplicate and, 24 hours later (^{18}F half-life, 109.8 minutes), PFK15 (25 mg/kg) was administered i.p. and the micro-PET scan was repeated 45 minutes later.

Xenograft studies

LLC, CT26, U-87, or BxPC-3 cells were collected from exponential growth phase culture in DMEM supplemented with 10% FCS. Cells were washed twice and resuspended in PBS (1×10^7 cells/mL). Groups of C57Bl6 (for LLC cells) or Balb/C athymic mice (for CT26, U-87 MG, or BxPC-3 cells; 20 g) were injected s.c. with 0.1 mL of the cell suspension (1×10^6 cells). Tumor masses were determined in a blinded fashion with Vernier calipers according to the following formula: mass(mg) = (width, mm)^2 × (length, mm)/2 (19) and then monitored daily with microcalipers. Mice bearing xenografts (150–200 mg) were then randomized to DMSO, PFK15 (25 mg/kg i.p. every 3 days × 4), irinotecan (70 mg/kg i.v. every 3 days × 4), temozolomide (30 mg/kg p.o. 3 days on 3 days off), or gemcitabine (100 mg/kg every 3 days × 4), and microcaliper measurements were conducted daily. All data are expressed as the mean ± SD of 2 experiments ($n = 8$ per group). Statistical significance was assessed by the unpaired 2 tail *T* test. In a separate series of experiments, LLC tumor-bearing mice were euthanized after only 4 days of treatment and the tumors were excised, fixed in formalin, embedded in paraffin, and stained with hematoxylin and eosin or with anticleaved caspase 3 (Abcam) using standard immunohistochemical methodologies.

Results

Identification of a more potent small molecule antagonist of PFKFB3

Initially, we synthesized 73 synthetic derivatives of 3PO and then examined their relative potency against the activity of recombinant human PFKFB3 protein. We identified a 3PO derivative in which a quinolinyl ring was substituted for a pyridinyl ring, 1-(4-pyridinyl)-3-(2-quinolinyl)-2-propen-1-one (PFK15; Fig. 1A), that displayed approximately 100-fold more activity against PFKFB3 than 3PO (IC_{50}: 3PO, 22.9 μmol/L; PFK15, 207 nmol/L; Fig. 1B). Subsequent computational modeling suggested that the increased activity of PFK15 may be due to the interaction of the quinolinyl ring with residues that

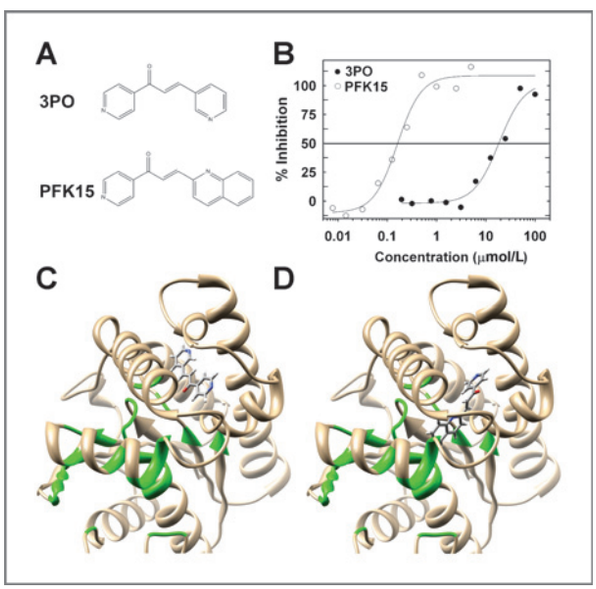

Figure 1. Identification of a novel small molecule antagonist of PFKFB3. A, structures of 3PO and the 3PO analogue PFK15. B, physical screening of 3PO and PFK15 for inhibitory effects on recombinant PFKFB3 activity. C, computational modeling of 3PO docked in the substrate-binding domain of PFKFB3 (green indicates ATP/ADP-interacting residues). D, computational modeling of PFK15 docked in the substrate-binding domain of PFKFB3.

form the ADP/ATP binding site of PFKFB3 (highlighted in green; compare Fig. 1C and D). We next examined PFK15 for activity against 96 kinases using a commercially available active site–dependent competition binding assay core service (KINOMEscanEDGE). This assay quantifies the capacity of test agents to compete with an immobilized, active site–directed ligand using a DNA-tagged kinase and immobilized ligand and compound. PFK15 had no significant inhibitory effect on any of the tested kinases (range = 93–100% of control; 10 μmol/L PFK15; see Materials and Methods to access names of 96 kinases). In addition, up to 100 μmol/L PFK15 was found to not inhibit the activities of purified PFK-1, hexokinase, phosphoglucose isomerase, or PFKFB4 (data not shown). These observations supported the specificity of PFK15 for PFKFB3 as well as the continued analysis of PFK15 for activity against the metabolism and viability of transformed cells.

Inhibition of cancer cell viability, F26BP, glucose uptake, and ATP by 3PO and PFK15

The parent compound 3PO suppresses the metabolism and growth of Jurkat T-cell leukemia cells at a relatively low concentration (18). To identify a lung adenocarcinoma cell line that is similarly sensitive, we employed the National Cancer Institute 60 cell line screening service that assesses the cytostatic/toxic effects of test agents on 59 cancer cell lines *in vitro* by measuring cellular protein content over 48 hours. H522 cells were found to be the most sensitive lung adenocarcinoma cell line (Table 1) and we thus elected to directly compare the metabolic effects of 3PO relative to PFK15 in these adenocarcinoma cells and Jurkat leukemia cells. Initially, we assessed the cytotoxic effects of 3PO relative to PFK15 on Jurkat and H522 cells after 48 hours and observed an increase in the potency of PFK15 [IC_{50}: Jurkat, 7.2 μmol/L (3PO), 2.42 μmol/L (PFK15); H522, 5.57 μmol/L (3PO), 0.72 μmol/L (PFK15); Fig. 2A and B). Suppression of PFK-1 activity is expected to increase the concentration of its substrate, F6P, which is in equilibrium with glucose 6-phosphate, a potent inhibitor of hexokinase and thus glucose uptake (which is dependent on phosphorylation by hexokinase). Not surprisingly, 3PO and heterozygous genomic deletion of the *Pfkfb3* gene reduce both the intracellular concentration of F26BP and glucose uptake of transformed cells *in vitro* and *in vivo* (refs. 14 and 18). We examined the steady-state concentration of the substrate of PFKFB3, F26BP, as well as 2-[1-^{14}C]-deoxy-D-glucose (^{14}C-2DG) uptake and intracellular ATP, after only 3 hours of PFKFB3 inhibitor exposure (before the detection of cytotoxicity). We found that both 3PO and PFK15 reduced F26BP, glucose uptake, and intracellular ATP but that PFK15 was more potent than 3PO (Fig. 2C–H). Interestingly, we found that the marked reduction of ATP caused by PFK15 could be partially rescued by pyruvate [PFK15-mediated ATP depletion (% control): 5 mmol/L glucose alone, 5.29 ± 0.85%; 5 mmol/L glucose + 1 mmol/L pyruvate, 45.62 ± 1.72%; P value = 0.0017]. In contrast, the ATP depletion caused by PFK15 could not be significantly reversed by the addition of either 10 mmol/L lactate or 4 mmol/L glutamine (data not shown). These observations provide indirect support for the hypothesis that PFK15 predominantly targets the glycolytic pathway and that the downstream add-back of pyruvate may

Table 1. Effect of PFK15 on the growth of cancer cell lines using the sulforhodamine B assay (GI_{50}; μmol/L; National Cancer Institute Developmental Therapeutics Program)

Leukemia		**Ovarian cancer**	
CCRF-CEM	3.80	IGROV1	4.37
HL-60(TB)	2.04	OVCAR-3	3.16
MOLT-4	2.24	OVCAR-4	2.34
RPMI-8226	2.19	OVCAR-5	5.37
SR	0.23	OVCAR-8	1.82
		NCI/ADR-RES	3.89
Non–small cell lung cancer		SK-OV-3	15.14
A549/ATCC	5.37	**Renal cancer**	
EKVX	12.88	786-0	2.00
HOP-62	2.34	A498	11.75
HOP-92	3.02	ACHN	2.04
NCI-H23	3.16	CAKI-1	11.48
NCI-H460	3.47	RXF 393	1.70
NCI-H522	1.74	SN12C	1.86
		TK-10	4.07
Colon cancer		UO-31	1.62
COLO 205	2.45		
HCC-2998	1.91	**Prostate cancer**	
HCT-116	1.32	PC-3	3.16
HCT-15	1.1	DU-145	2.24
HT29	2.51		
KM12	1.95	**Breast cancer**	
SW-620	1.7	MCF7	1.86
		MDA-MB-231/ ATCC	2.04
CNS cancer		HS 578T	20.89
SF-268	5.25	BT-549	2.75
SF-295	13.49	T-47D	3.63
SF-539	2.51	MDA-MB-468	1.66
SNB-19	4.57		
SNB-15	11.22		
U251	2.04		
Melanoma			
LOX IMVI	1.66		
MALME-3M	3.31		
M14	3.72		
MDA-MB-435	3.24		
SK-MEL-2	6.46		
SK-MEL-28	2.09		
SK-MEL-5	3.47		
UACC-257	3.98		
UACC-62	2.51		

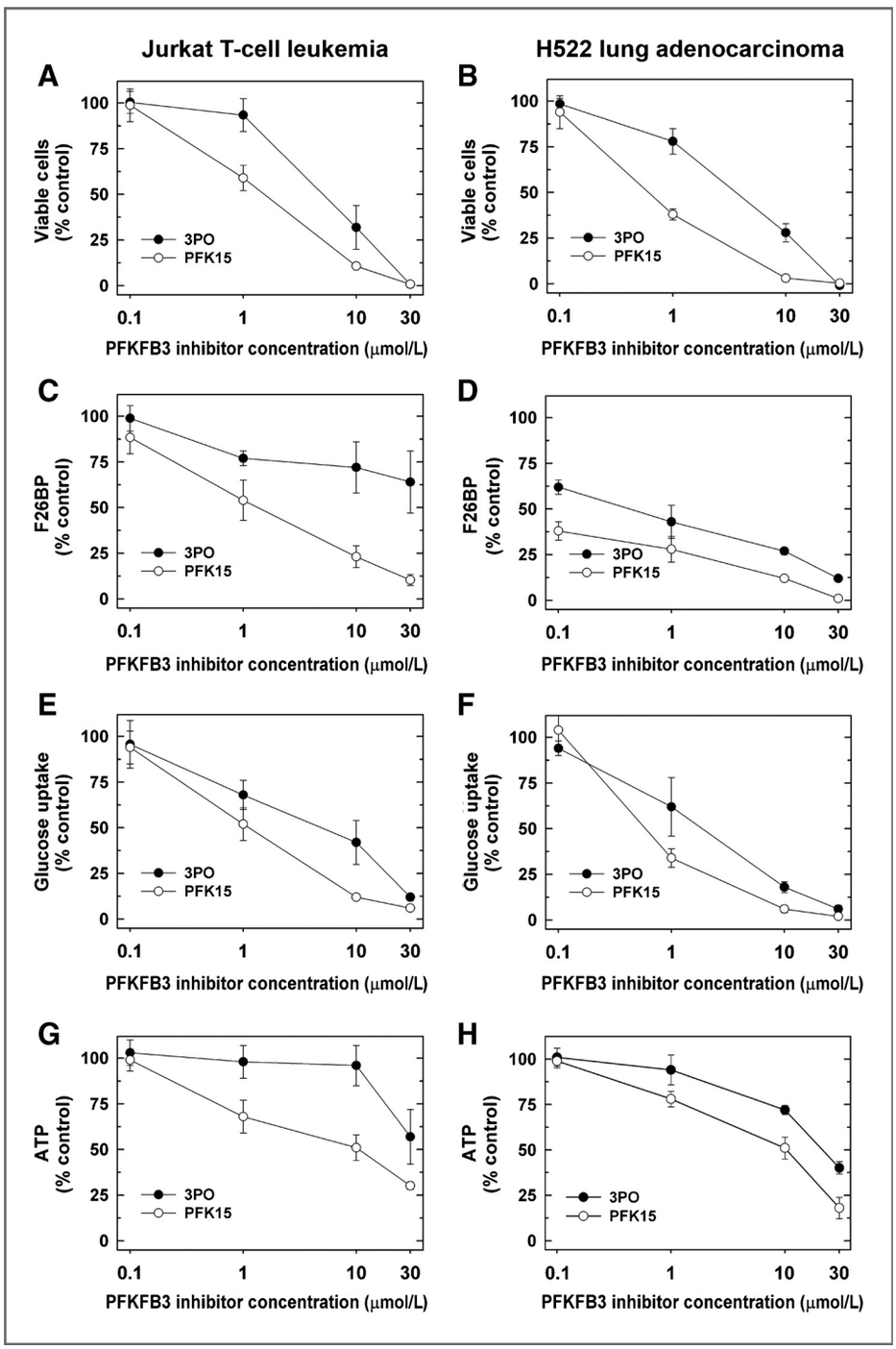

Figure 2. Effects of 3PO and PFK15 on the viability, F26BP, glucose uptake, and intracellular ATP of Jurkat T-cell leukemia cells and H522 lung adenocarcinoma cells. Jurkat or H522 cells grown in exponential phase were exposed to the indicated concentrations of 3PO or PFK15 and, after 48 hours, the effects on viability were determined (A and B). To identify acute effects on known metabolic effects of PFKFB3 inhibition, the Jurkat and H522 cells were exposed to 3PO or PFK15 for 3 hours and the F26BP (C and D), 2-[1-^{14d}C]-deoxy-D-glucose uptake (E and F), and intracellular ATP (G and H) were measured.

provide a source of carbons necessary for the TCA cycle as well as a mechanism to provide NAD+ via LDH-A.

3PO and PFK15 cause apoptosis in Jurkat T-cell leukemia cells

In previous studies, we found that 3PO suppressed cell proliferation and, at >10 μmol/L concentrations, caused cell death via undefined mechanisms (18). Because glucose deprivation can induce apoptosis (20), we postulated that the reduction in glucose uptake caused by 3PO and the more potent PFK15 might induce apoptotic death in these cells. Using 25 μmol/L etoposide as a positive control, we directly compared the effects of 2 concentrations of 3PO and PFK15 (3 and 20 μmol/L to encompass both limited and extensive cell death) on early (Annexin V+/PI−) and late (Annexin V+/PI+) apoptosis using

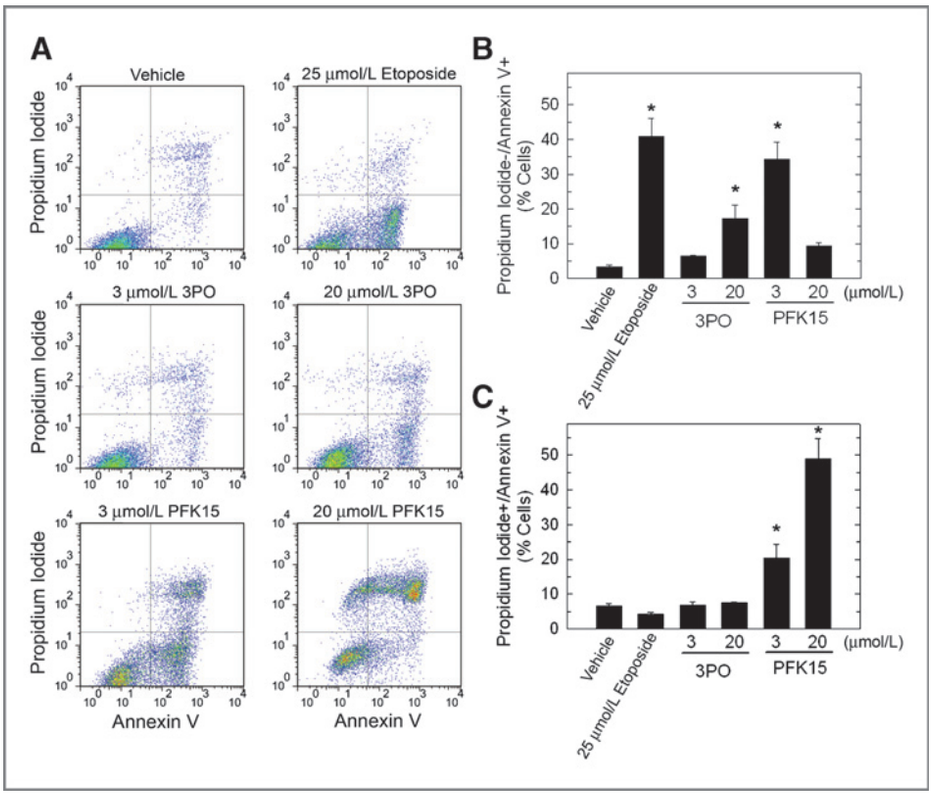

Figure 3. PFKFB3 inhibitors induce apoptosis in Jurkat T-cell leukemia cells. A, Jurkat cells were exposed to the indicated concentrations of etoposide, 3PO or PFK15 for 5 hours, stained for Annexin V and PI and analyzed by flow cytometry. The percentages of Annexin V+/PI− (early apoptotic; B) and Annexin V+/PI+ (late apoptotic; C) cells relative to the total population were quantified. *, $P < 0.01$.

flow cytometry. After 5 hours of exposure, we found that whereas 20 μmol/L 3PO and 3 μmol/L PFK15 increased the number of cells undergoing early apoptosis (Fig. 3A and B), both 3 and 20 μmol/L PFK15 caused a dose-dependent increase in the number of cells already undergoing late apoptosis (Fig. 3A and C). These observations provide the first demonstration that this class of PFKFB3 inhibitors can induce apoptosis in transformed cells and suggest that PFK15 causes a more rapid progression to late apoptosis than 3PO.

PFK15 displays improved pharmacokinetic properties relative to 3PO

A key objective of our pursuit to identify a clinical candidate that inhibits PFKFB3 has been to improve the pharmacokinetic properties of the parent compound 3PO. We i.v. administered 3PO or PFK15 to C57Bl/6 mice and then, using LC/MS-MS, assessed the plasma concentration of each of the compounds over time. PFK15 displayed a marked reduction in clearance (3PO = 2312 mL/min/kg; PFK15 = 46.2 mL/min/kg) simultaneously with increased $T_{1/2}$ (3PO = 0.3 h; PFK15 = 5.1 h), C_{max} (3PO = 113 ng/mL; PFK15 = 3053 ng/mL) and $AUC_{0\text{-inf}}$ (3PO = 36 ng/h/mL; PFK15 1804 ng/h/mL). Microsomes are membrane vesicles isolated from hepatocyte smooth endoplasmic reticulum that contain multiple enzymes required to metabolize drugs including cytochrome P450s, flavin-containing monooxygenases, and uridine 5′-diphospho (UDP) glucuronyl transferases. Human microsome stability of PFK15 was prolonged relative to 3PO providing a potential mechanism for the observed improvements in pharmacokinetic properties [3PO = 1.9 min (100%); PFK15 = 2.9 min (100%)]. These data indicate that the substitution of the pyridinyl ring in 3PO with a quinolinyl ring provides a useful platform for the development of PFKFB3 inhibitors with improved pharmacokinetic properties.

PFK15 suppresses the growth of LLC xenografts

Intraperitoneal administration of 25 mg/kg PFK15 every 3 days caused <10% body mass loss and no end organ toxicity based on blood, urine, and histological analyses. Because 25 mg/kg of PFK15 was easily administered in a small volume despite the limited solubility of PFK15, this nontoxic dose and schedule was selected for the efficacy testing in xenograft and syngeneic models of tumorigenesis. We initially examined the relative effects of daily intraperitoneal administration of PFK15 on the growth of established LLC tumors *in vivo*. Although we did not observe tumor regression as a result of PFK15 administration, we did observe a statistically significant reduction in the growth of the LLC tumors (Fig. 4A) without a major effect on body mass (Fig. 4B). Importantly, although LLC cells are well established to metastasize from the subcutaneous tumors to the lungs, no lung metastases were identified in the LLC-bearing mice that had been treated with PFK15 (Fig. 4C). We then examined a subset of tumors for F26BP and apoptotic cells 4 days after initiation of

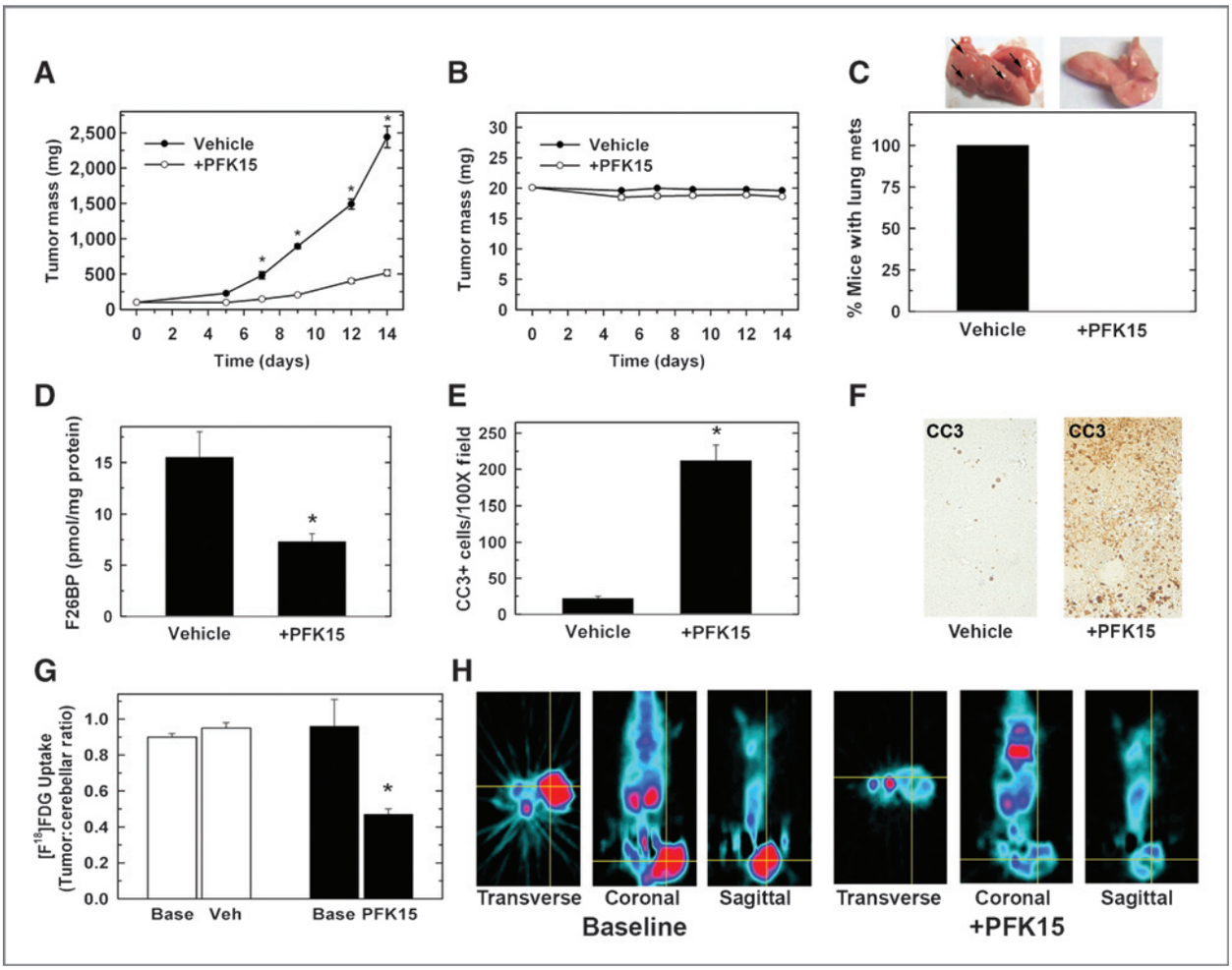

Figure 4. PFK15 suppresses the growth, metastatic spread, and glucose metabolism of LLC tumors in syngeneic mice. Groups of 8 C57Bl/6 mice (20 g) were injected s.c. with 0.1 mL of an LLC cell suspension (1×10^6 cells) and tumor masses were determined in a blinded fashion with Vernier calipers. Mice bearing xenografts (150–200 mg) then were randomized to DMSO or PFK15 and microcaliper measurements (A) and body mass (B) were collected daily. After 14 days, mice were euthanized and the lungs were examined for metastases (C). Tumors were extracted in a separate subgroup of mice after 4 days and analyzed for F26BP (D) and cleaved caspase 3 expression as a measure of apoptosis (E and F). A separate cohort of tumor-bearing mice underwent baseline micro-PET imaging of FDG uptake and, 24 hours later, were administered PFK15 (25/kg i.p. once) and the micro-PET scan was repeated in 45 minutes. Regions of interest in the tumor and cerebellum were quantified in quadruplicate (G) and a representative cut is provided in the transverse, coronal, and sagittal views (H). *, $P < 0.01$.

PFKFB3 inhibitor administration ($n = 4$). We found that PFK15 reduced tumor-associated F26BP (Fig. 4D) and caused a marked increase in the number of cells that were positive for cleaved caspase 3 by immunohistochemistry (Fig. 4E and F). Taken together, these results suggest that PFK15 can reduce tumor growth and induce apoptosis *in vivo*, is well tolerated in terms of body mass and has the unanticipated ability to prevent either the initiation or growth of metastases.

PFK15 suppresses ^{18}F-FDG uptake by LLC xenografts

We postulated that PFK15 would acutely attenuate the glucose uptake of xenografted tumors *in vivo*. We conducted baseline ^{18}F-FDG-PET imaging of LLC-bearing C57Bl/6 mice and, 24 hours later, injected PFK15 and then reimaged the LLC-bearing mice after 45 minutes. We observed a ~50% reduction in ^{18}F-FDG uptake after PFK15 administration normalized to the FDG uptake in the cerebellum (neurons do not express PFKFB3 protein; Fig. 4G and H). These data show that PFK15 selectively suppresses glucose uptake by tumors *in vivo* and suggest that FDG uptake scans may be a useful pharmacodynamic endpoint of PFKFB3 inhibitors in clinical trials.

PFK15 displays antitumor activity that is similar to commonly used chemotherapeutic agents

Finally, we directly compared the antitumor effects of PFK15 to 3 chemotherapeutic agents that are U.S. Food and Drug Administration (FDA)-approved for the treatment of human cancers. We found that PFK15 suppressed

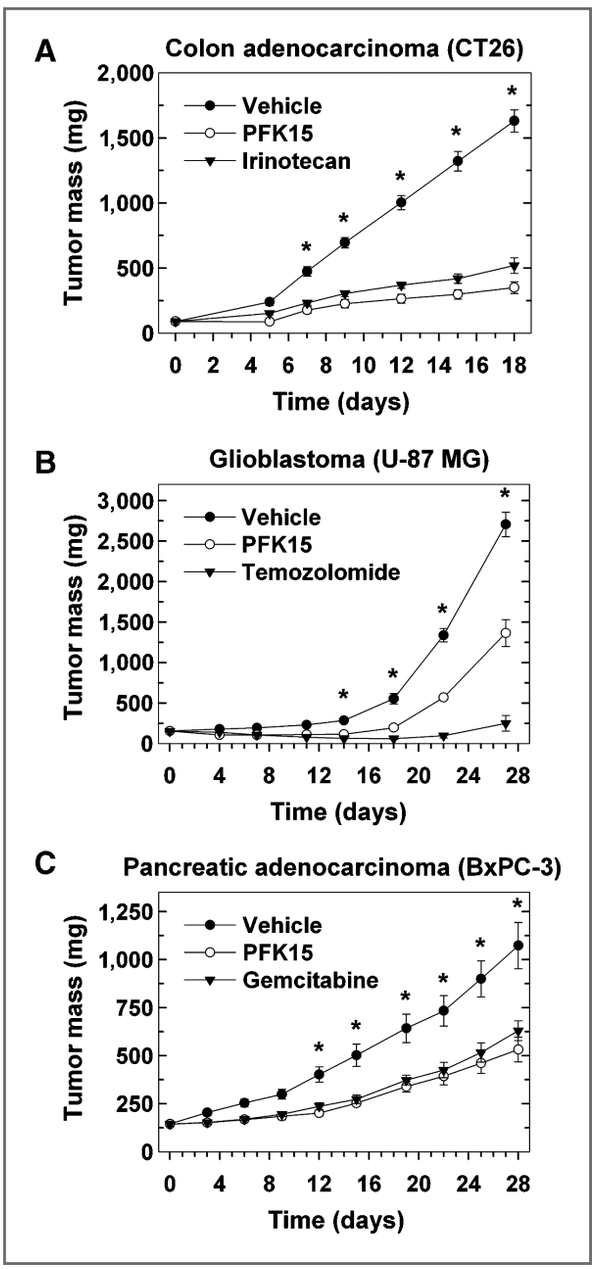

Figure 5. PFK15 suppresses the growth of several human xenograft tumors in athymic mice. Groups of eight athymic mice (20 g) were injected s.c. with CT26 (A), U-87 MG (B), and BxPC-3 (C) cells and tumor masses were determined in a blinded fashion with Vernier calipers. Mice bearing xenografts (150–200 mg) were then randomized to DMSO, the indicated standard chemotherapy, or PFK15 and the tumor masses were quantified with microcalipers. *, $P < 0.01$.

the growth of colon and pancreatic adenocarcinomas similarly to irinotecan (Fig. 5A) and gemcitabine (Fig. 5C), respectively. However, the activity of PFK15 against glioblastoma growth was lower than that observed by temozolomide (Fig. 5B). These preclinical studies raise the prospect that PFK15 and close synthetic derivatives may show cytotoxic activity against human cancers in clinical trials.

Discussion

In this study, we describe the development of a novel small molecule antagonist of PFKFB3 that suppresses the glucose uptake and viability of human cancer cell lines *in vitro* and that has improved pharmacokinetic properties relative to the parent compound 3PO mice. Importantly, PFK15 rapidly reduces F26BP and glucose uptake and induces apoptosis in cancer cells *in vitro* and *in vivo*, indicating that these metabolic measures can be used as pharmacodynamic endpoints in clinical trials. This study provides indirect support for a catastrophic cascade in which suppression of PFKFB3 activity reduces the steady-state concentration of F26BP, which, in turn, causes suppression of PFK-1 activity and glucose uptake. Although the precise mechanism for the effect of PFK15 on glucose uptake has not been determined, we postulate that certain glycolytic intermediates upstream of PFK-1 may allosterically inhibit hexokinase or affect the glucose transporters. Importantly, the effect of PFKFB3 inhibition on glucose uptake has been well established by the observation that heterozygous genomic deletion of the *Pfkfb3* gene reduces the intracellular F26BP and glucose uptake of transformed cells *in vitro* and *in vivo* (14). Given that withdrawal of glucose from transformed cells and resultant ATP depletion induces apoptosis (20), we postulate that the observed reduction of glucose uptake and intracellular ATP caused by PFK15 may cause apoptosis via similar yet undefined mechanisms. Importantly, we also believe that the functional glucose starvation that PFK15 causes via PFKFB3 inhibition also results in carbon depletion, which in turn leads to disruptions in multiple anabolic pathways that may not be readily circumvented by discrete resistance-causing mutations. Finally, given the potent antiglycolytic effects of PFK15, we also hypothesize that this class of compounds will prove useful for the targeting of resistant hypoxic cancer cells as well as the development of combinatorial strategies to suppress growth using PFK15 with ionizing radiation.

Although we found that PFK15 was more potent than 3PO at inhibiting recombinant PFKFB3 activity, glucose uptake, intracellular F26BP, and ATP, the increased potency of PFK15 related to apoptosis was dramatically greater than that observed with the metabolic changes. We suspect that relatively small increments in the suppressive activity of PFK15 on glucose uptake and intracellular ATP may reach a threshold that results in a much larger effect on apoptosis depending on the cell type, availability of alternative substrates, such as glutamine and pyruvate, and on oxygen availability *in vivo*. An alternative and certainly plausible explanation relates to potential off-target effects of PFK15 on mitochondrial metabolism and integrity. However, ectopic expression of PFKFB3 has previously been shown to increase intracellular F26BP and protect Jurkat T-cell leukemia cells from the cytotoxic effects of the parent compound, 3PO, indicating that

PFKFB3 is, at a minimum, an essential enzyme target of this class of small molecules (18).

These preclinical studies have facilitated the design of the first-in-human phase I clinical trial of a PFK15 derivative similarly modified with a quinolinyl ring in advanced solid tumor patients. The original parent compound 3PO was recently reported to have potent activity against a highly relevant mouse model of leukemia (21) and we thus anticipate that once the maximum tolerated dose is identified, phase II trials of the optimized PFKFB3 inhibitor also will be proposed in patients suffering from leukemias. Perhaps more importantly, we expect the development of multiple phase I/II trials in which PFKFB3 inhibitors are combined with FDA-approved agents that are the standard of care for distinct cancer types as well as the rational combination of PFKFB3 inhibitors with agents that suppress angiogenesis, electron transport chain activity, glutamine metabolism, and autophagy.

Recently, we showed that PFKFB3 expression and F26BP synthesis are increased by stimulation of human $CD3^+$ T cells and that 3PO suppresses the activation of T cells *in vitro* and *in vivo* (22). In addition, PFKFB3 was initially identified in the mid-1990s as an inducible PFK-2 (iPFK-2) isozyme that is rapidly induced by endotoxin in human macrophages (23, 24). Given our growing understanding of the immunosuppressive effects of regulatory T cells (25) and myeloid-derived suppressor cells (26) and the differential metabolic requirements of various T-cell subsets (27), we speculate that PFKFB3 inhibitors may have unidentified pleiotropic effects on the immune system that may contribute to their antitumor properties. Conditional *Pfkfb3* knockout mice in which the expression of Cre is controlled by transcription factors that are immune lineage-specific should enable a more complete characterization of the roles of PFKFB3 in the activation of distinct suppressor lineages of cells involved in tumor immunity.

In conclusion, we describe the identification of a novel PFKFB3 inhibitor that has acceptable pharmacokinetic properties, on-target metabolic effects and antitumor activity in 4 mouse models of cancer. Coupled with the identification of potential biomarkers for activity, we believe that the results of this study provide essential rationale for the continued testing of this novel class of targeted therapeutic agents in clinical trials.

Disclosure of Potential Conflicts of Interest

No potential conflicts of interest were disclosed.

Authors' Contributions

Conception and design: J. O'Neal, G. Tapolsky, D.M. Miller, J.O. Trent, J. Chesney
Development of methodology: B.F. Clem, S. Telang
Acquisition of data (provided animals, acquired and managed patients, provided facilities, etc.): B.F. Clem, J. O'Neal, G. Tapolsky, A.L. Clem, S. Telang, J. Chesney
Analysis and interpretation of data (e.g., statistical analysis, biostatistics, computational analysis): B.F. Clem, J. O'Neal, G. Tapolsky, Y. Imbert-Fernandez, A. Klarer, J. Chesney
Writing, review, and/or revision of the manuscript: B.F. Clem, J. O'Neal, G. Tapolsky, D.A. Kerr, R. Redman, S. Telang, J. Chesney
Administrative, technical, or material support (i.e., reporting or organizing data, constructing databases): A.L. Clem, J. Chesney
Study supervision: J. Chesney

Grant Support

This work was supported by NIH/NCRR 3P20RR018733-09 (B.F. Clem), Breast CDMRP 10903731 (J. O'Neal), and NIH/NCI 1RO1CA149438 (J. Chesney).

The costs of publication of this article were defrayed in part by the payment of page charges. This article must therefore be hereby marked *advertisement* in accordance with 18 U.S.C. Section 1734 solely to indicate this fact.

Received February 7, 2013; revised April 9, 2013; accepted April 30, 2013; published OnlineFirst May 14, 2013.

References

1. Vallabhajosula S. (18)F-labeled positron emission tomographic radiopharmaceuticals in oncology: an overview of radiochemistry and mechanisms of tumor localization. Semin Nucl Med 2007;37:400–19.
2. Castell F, Cook GJ. Quantitative techniques in 18FDG PET scanning in oncology. Br J Cancer 2008;98:1597–601.
3. Semenza GL. Hypoxia-inducible factors: mediators of cancer progression and targets for cancer therapy. Trends Pharmacol Sci 2012;33:207–14.
4. Dang CV, Le A, Gao P. MYC-induced cancer cell energy metabolism and therapeutic opportunities. Clin Cancer Res 2009;15:6479–83.
5. Osthus RC, Shim H, Kim S, Li Q, Reddy R, Mukherjee M, et al. Deregulation of glucose transporter 1 and glycolytic gene expression by c-Myc. J Biol Chem 2000;275:21797–800.
6. Shim H, Dolde C, Lewis BC, Wu CS, Dang G, Jungmann RA, et al. c-Myc transactivation of LDH-A: implications for tumor metabolism and growth. Proc Natl Acad Sci U S A 1997;94:6658–63.
7. Van Schaftingen E, Jett MF, Hue L, Hers HG. Control of liver 6-phosphofructokinase by fructose 2,6-bisphosphate and other effectors. Proc Natl Acad Sci U S A 1981;78:3483–6.
8. Yalcin A, Telang S, Clem B, Chesney J. Regulation of glucose metabolism by 6-phosphofructo-2-kinase/fructose-2,6-bisphosphatases in cancer. Exp Mol Pathol 2009;86:174–9.
9. Van Schaftingen E, Hue L, Hers HG. Fructose 2,6-bisphosphate, the probably structure of the glucose- and glucagon-sensitive stimulator of phosphofructokinase. Biochem J 1980;192:897–901.
10. Minchenko O, Opentanova I, Caro J. Hypoxic regulation of the 6-phosphofructo-2-kinase/fructose-2,6-bisphosphatase gene family (PFKFB-1-4) expression *in vivo*. FEBS Lett 2003;554:264–70.
11. Obach M, Navarro-Sabate A, Caro J, Kong X, Duran J, Gomez M, et al. 6-Phosphofructo-2-kinase (pfkfb3) gene promoter contains hypoxia-inducible factor-1 binding sites necessary for transactivation in response to hypoxia. J Biol Chem 2004;279:53562–70.
12. Garcia-Cao I, Song MS, Hobbs RM, Laurent G, Giorgi C, de Boer VC, et al. Systemic elevation of PTEN induces a tumor-suppressive metabolic state. Cell 2012;149:49–62.
13. Manes NP, El-Maghrabi MR. The kinase activity of human brain 6-phosphofructo-2-kinase/fructose-2,6-bisphosphatase is regulated via inhibition by phosphoenolpyruvate. Arch Biochem Biophys 2005;438:125–36.
14. Telang S, Yalcin A, Clem AL, Bucala R, Lane AN, Eaton JW, et al. Ras transformation requires metabolic control by 6-phosphofructo-2-kinase. Oncogene 2006;25:7225–34.
15. Atsumi T, Chesney J, Metz C, Leng L, Donnelly S, Makita Z, et al. High expression of inducible 6-phosphofructo-2-kinase/fructose-2,6-

bisphosphatase (iPFK-2; PFKFB3) in human cancers. Cancer Res 2002;62:5881–7.
16. Chesney J, Telang S, Yalcin A, Clem A, Wallis N, Bucala R. Targeted disruption of inducible 6-phosphofructo-2-kinase results in embryonic lethality. Biochem Biophys Res Commun 2005;331:139–46.
17. Herrero-Mendez A, Almeida A, Fernandez E, Maestre C, Moncada S, Bolanos JP. The bioenergetic and antioxidant status of neurons is controlled by continuous degradation of a key glycolytic enzyme by APC/C-Cdh1. Nat Cell Biol 2009;11:747–52.
18. Clem B, Telang S, Clem A, Yalcin A, Meier J, Simmons A, et al. Small-molecule inhibition of 6-phosphofructo-2-kinase activity suppresses glycolytic flux and tumor growth. Mol Cancer Ther 2008;7:110–20.
19. Taetle R, Rosen F, Abramson I, Venditti J, Howell S. Use of nude mouse xenografts as preclinical drug screens: *in vivo* activity of established chemotherapeutic agents against melanoma and ovarian carcinoma xenografts. Cancer Treat Rep 1987;71:297–304.
20. El Mjiyad N, Caro-Maldonado A, Ramirez-Peinado S, Munoz-Pinedo C. Sugar-free approaches to cancer cell killing. Oncogene 2012;30: 253–64.
21. Reddy MM, Fernandes MS, Deshpande A, Weisberg E, Inguilizian HV, Abdel-Wahab O, et al. The JAK2V617F oncogene requires expression of inducible phosphofructokinase/fructose-bisphosphatase 3 for cell growth and increased metabolic activity. Leukemia 2012;26:481–9.
22. Telang S, Clem BF, Klarer AC, Clem AL, Trent JO, Bucala R, et al. Small molecule inhibition of 6-phosphofructo-2-kinase suppresses t cell activation. J Transl Med 2012;10:95.
23. Chesney J, Mitchell R, Benigni F, Bacher M, Spiegel L, Al-Abed Y, et al. An inducible gene product for 6-phosphofructo-2-kinase with an AU-rich instability element: role in tumor cell glycolysis and the Warburg effect. Proc Natl Acad Sci U S A 1999;96:3047–52.
24. Marsin AS, Bouzin C, Bertrand L, Hue L. The stimulation of glycolysis by hypoxia in activated monocytes is mediated by AMP-activated protein kinase and inducible 6-phosphofructo-2-kinase. J Biol Chem 2002;277:30778–83.
25. Jacobs JF, Nierkens S, Figdor CG, de Vries IJ, Adema GJ. Regulatory T cells in melanoma: the final hurdle towards effective immunotherapy? Lancet Oncol 2012;13:e32–42.
26. Montero AJ, Diaz-Montero CM, Kyriakopoulos CE, Bronte V, Mandruzzato S. Myeloid-derived suppressor cells in cancer patients: a clinical perspective. J Immunother 2012;35:107–15.
27. Wang R, Dillon CP, Shi LZ, Milasta S, Carter R, Finkelstein D, et al. The transcription factor Myc controls metabolic reprogramming upon T lymphocyte activation. Immunity 2011;35:871–82.